

Sliding window and compressive sensing for low-field dynamic magnetic resonance imaging

Cristian Toraci, Gabriele Zaccaria, Stefano Ceriani, David Wilson, Marco Fato, and Michele Piana

Abstract—We describe an acquisition/processing procedure for image reconstruction in dynamic Magnetic Resonance Imaging (MRI). The approach requires sliding window to record a set of trajectories in the k-space, standard regularization to reconstruct an estimate of the object and compressed sensing to recover image residuals. We validated this approach in the case of specific simulated experiments and, in the case of real measurements, we showed that the procedure is reliable even in the case of data acquired by means of a low-field scanner.

Index Terms—Dynamic MRI; sliding window; regularization; compressed sensing.

I. INTRODUCTION

Magnetic resonance imaging (MRI) is a tomographic technique that produces images of some internal chemical characteristic of an object from induced nuclear magnetic resonance signals. Many clinical applications in MRI involve imaging of non-static anatomies, like in the case of abdominal and cardiac imaging, while other applications can take advantages from dynamic imaging of objects in motion, like in the case of studies of joint kinematics.

The signal generated by an MRI system is the Fourier transform of the image of interest, sampled on a finite portion of the spatial frequencies using a limited number of points. The region that must be acquired to reconstruct a given image with the desired spatial resolution is usually called *k-space*: k-space data are acquired along continuous trajectories whose length is limited by sampling bandwidth and signal decay due to relaxation. The acquisition time of a whole MRI exam is roughly proportional to the number of sampled trajectories. Therefore, in dynamic imaging, this number should be optimized to realize a trade-off between undersampling and motion blur artifacts. To address this issue several strategies have been proposed:

- Historically, Echo Planar Imaging (EPI) [1]–[3] allows full coverage of the k-space in a very short time (40 to 100 ms) thus reducing motion-related artifacts. Its main drawbacks are the use of demanding hardware characteristics and notable geometric distortions induced by inhomogeneities of the static magnetic field.

C. Toraci is with the IRCCS San Martino IST, Genova, Italy and the Dipartimento di Matematica, Università di Genova, Genova, Italy

G. Zaccaria is with the Dipartimento di Matematica, Università di Genova, Genova, Italy

M. Piana is with the Dipartimento di Matematica, Università di Genova, Genova, Italy and CNR - SPIN, Genova

D. Wilson is with the Department of Orthopaedics and the Centre for Hip Health and Mobility at the University of British Columbia and Vancouver Coastal Health Research Centre

M. Fato and S. Ceriani are with the Dipartimento di Informatica, Bioingegneria, Robotica e Ingegneria dei Sistemi, Università di Genova, Genova, Italy

- Parallel imaging [4], [5] utilizes phase-array coils whose receiving elements have a characteristic space-dependent sensitivity distribution. The redundancy given by multiple elements can be used to reconstruct under-sampled data. In parallel imaging, however, there are limitations due to the kind of acquisition protocol and hardware adopted such as signal-to-noise (SNR) ratio, image geometry or maximal achievable acceleration factors.
- A more general approach comes from constrained reconstruction techniques that aim at integrating partial k-space data using *a-priori* information [6]. These might be a high resolution reference image, acquired before or after the fast acquisition, or some known property of the image, like sparsity in a proper basis.

In this last framework, compressed sensing [7], [8] provides computational tools able to reconstruct sparse signals from an under-sampled set of measurements. Although MRI images are not in general sparse, sparsifying transforms can be introduced [9], [10]. For example, kt-FOCUSS [11] records one or two fully sampled data sets and several under-sampled data sets. Then RIGR [12] or motion estimation and compensation techniques used in video encoding [13] are applied to compute initial *estimates* for all the time samples; finally, sparsification is used for reconstructing the difference (*residuals*) between optimal images and estimates. The main drawback of kt-FOCUSS is in the fact that recording high-resolution volumes requires a long acquisition time and thus notably limits the applicability of the method in the clinical workflow.

The goal of the present paper is to apply compressed sensing in order to reconstruct dynamic MRI volumes without the time-demanding acquisition of high resolution data. An example of this approach is given in [14], where sparsification is achieved by differentiating along the temporal direction. We observe that numerical differentiation is numerically unstable. This drawback is not an issue for [14], where data acquired by means of a high-field MRI scanner are used. Here we are interested in applications at low-field data and in this case the low signal-to-noise ratio may impact on the reconstruction quality. Therefore we realize this approach by means of a different sparsification scheme and show its effectiveness in the case of data at 0.5 T. More specifically, in such scheme:

- 1) A sliding window approach [15] records a set of trajectories of the body in k-space.
- 2) A Fourier-based inversion technique provides a first estimate of the object, which is affected by motion blur, by utilizing a high enough number of trajectories.
- 3) A kt-FOCUSS-like approach uses this blurred estimate and compressed sensing to reconstruct the residuals.

- 4) Summing up the residuals and the estimates provides a set of images, each one corresponding to a very limited number of trajectories (and therefore to a very limited temporal range in the acquisition time).

We observe that, in item 2), the computation of the estimate uses fully or nearly-fully sampled data and can be realized by using standard regularization methods for image reconstruction. On the other hand, item 3) relies on the fact that de-blurring can be realized using compressed sensing as shown in [16]. As far as the implementation of the compressed sensing step is concerned, we observe that the identification of the optimal technique in this field is still an open research issue and therefore we decided to compare the performances provided by two different methods: Orthogonal Matching Pursuit (OMP) [17], that recovers the sparse components of the image in a *greedy* fashion, thus limiting the computational effort of the processing; and an optimization method with ℓ_1 penalty term where the minimum problem is solved by using a split-Bregman algorithm.

The content of the paper is organized as follows. In Section II we describe the imaging model and the reconstruction strategy. Section III contains the details of the method implementation. Section IV contains some numerical results using synthetic data simulated according to realistic procedures and Section V shows how this procedure works in the case of a set of experimental measurements of the cervical spine. Our conclusions are offered in Section VI.

II. MODEL AND RECONSTRUCTION STRATEGY

Data formation in MRI can be mathematically modeled by means of a Fourier transform relation. More precisely, at a given acquisition time, MRI records samples of the Fourier transform of the function of interest along trajectories in the k-space. At the end of a sequence of acquisition times, the data is represented by a set of trajectories. More formally, let $x \in \mathbb{C}^{N \times N}$ be a discretized version of the function representing the object of interest (i.e., x is the unknown in the image space) and $y \in \mathbb{C}^{M \times K}$ is the measured data (i.e., in the k-space, a set of M trajectories made of K sampled frequencies): then, using a lexicographic ordering, y and x are related by the matrix equation

$$y = Fx, \quad (1)$$

where $F \in \mathbb{C}^{MK \times N^2}$ is a linear transformation obtained from a (non-uniform) discretization of the Fourier transform.

The MRI reconstruction problem is the one to determine an estimate of x given y . In the case of static imaging, if the number of trajectories M is high enough and the criterion with which they sample the k-space is Nyquist-like, this image reconstruction problem is well-posed and inverse Fourier transform provides reliable results. However, full (or high) k-space coverage requires a long acquisition time which implies, for dynamic studies, that images obtained by means of Fourier-based methods are affected by motion blur. On the other hand, motion blur can be reduced by using fewer trajectories but in this case other artifacts are introduced, that are due to the limited number of Fourier components one utilizes for the inversion. A computational strategy based on

compressed sensing may help to overtake this deadlock. Let us denote with y_ν the set of ν trajectories acquired in a time interval δt around time t . Then the reconstruction x_ν corresponding to y_ν can be written as

$$x_\nu = x_M + \delta x, \quad (2)$$

where x_M is the reconstruction obtained by applying some regularization method to the data y_M corresponding to the complete set of M trajectories. If F_ν is the linear transformation producing the ν trajectories from a given input data, we have that

$$F_\nu x_\nu = F_\nu x_M + F_\nu \delta x. \quad (3)$$

Assuming that δx is sufficiently sparse justifies the application of the constrained minimum problem

$$\begin{cases} \min \|\delta x\|_1 \\ \|F_\nu \delta x - (y_\nu - F_\nu x_M)\|_2^2 < \epsilon, \end{cases} \quad (4)$$

with ϵ sufficiently small. In order to implement such reconstruction strategy, three issues must be addressed:

- The data sets y_M and y_ν must have specific properties: M must be sufficiently big such that the corresponding estimate x_M is not affected by artifacts due to under-sampling the k-space; further, y_ν must be appropriate to compressed sensing, i.e. the corresponding δx must be sufficiently sparse and the undersampling must be lower near the center of k-space and higher near the periphery [9].
- In equation (4) both δx and x_M are unknown. Therefore a regularization method must be applied in order to reconstruct the estimate x_M .
- Once x_M has been reconstructed, a computational method is required to solve the constrained minimum problem (4) enhancing the sparsity of the solution.

In the following section we provide details about the implementation of the previous issues as adopted in the numerical applications.

III. IMPLEMENTATION

The reconstruction paradigm formulated in this paper requires a specific acquisition strategy, which is based on a sliding window scheme [18]. Let $k_m : [0, \tau] \rightarrow [-\pi, \pi]^2$ be a sampling trajectory in the two-dimensional k-space, such that $k_m(t)$ is the parametric representation of the m -th trajectory, t runs in the interval $[0, \tau]$ and τ is the acquisition time specific for that trajectory. Further, assume that the time required to sample a trajectory is short enough to have negligible motion in this interval. Then choose a set of trajectories $\{k_m\}_{m=1}^M$ in such a way that:

- 1) The set $k_{m_1} \cap k_{m_2}, \forall m_1 \neq m_2; m_1, m_2 = 1, \dots, M$ is made of a small number of frequencies.
- 2) The sampling of the k-space given by $\cup_{m=1}^M k_m$ is appropriate for solution of (1) by means of some regularization technique.
- 3) For some integer $\nu, 0 < \nu < M$, the sampling given by $\cup_{m=m_0-\nu/2}^{m_0+\nu/2} k_m$ is appropriate for inversion by means

of a compressed sensing technique for all m_0 such that $1 + \nu/2 \leq m_0 \leq M - \nu/2$.

Items 1) and 2) imply that the k-space is sampled in a complete way, so that the data y_M corresponding to $\cup_{m=1}^M k_m$ provide a good (but blurred) estimate x_M by means of some conventional inversion technique. Specifically, in our applications we utilized a Conjugate Gradient scheme to solve the weighted least-squares problem

$$x_M = \arg \min_x \|F^W x - y_M^W\|_2^2 \quad (5)$$

applied against a windowed version y_M^W of the data y_M . The windowed data is defined as follows: if y_m represents the data from trajectory k_m , then $y_m^W = y_m h_M(m)$, with h_M the Hamming window defined as $h_M(m) = 0.54 - 0.46 \cos(2\pi m/M)$. Analogously, $F^W = WF$ where W is a diagonal matrix whose non-zero entries are given by $h_M(m)$ for $m = 1, \dots, M$.

On the other hand, item 3) is not specific of sliding window but it is necessary for a compressed sensing approach to the reconstruction of the residual δx . In fact, once x_M is determined by (5), we computed δx by solving (4) with two methods: an Orthogonal Matching Pursuit (OMP) algorithm and an ℓ_1 optimization method.

A. Orthogonal Matching Pursuit

OMP is an iterative scheme that implements sparsity enhancement according to a *greedy* fashion. The main idea is based on the observation that a signal with s non-zero components generates data which are the linear combination of just s columns of the matrix modeling the data formation. The task of OMP is to iteratively select the column which is mostly correlated with the data and solve the reconstruction problem using just the selected columns.

In order to improve the speed of the method, in the numerical applications described in the next section we applied a modification of OMP, named KOMP (i.e., K -fold Orthogonal Matching Pursuit) [19] whereby, each iteration step chooses the $K > 1$ most correlated columns. It can be proved that this modification has the same convergence properties of OMP [20], [21]. At each iteration step, the reconstruction problem limited to the selected columns is solved by means of a Conjugate Gradient algorithm.

B. ℓ_1 optimization

Equation (4) can be determined by recasting it as the minimum problem

$$\delta x = \arg \min_{\delta x} \|F_\nu \delta x - (y_\nu - F_\nu x_M)\|_2^2 + \lambda \|\delta x\|_1 \quad (6)$$

where λ plays the role of a regularization parameter. In our applications this problem is solved by using the split-Bregman method [22] which transforms equation (6) into the new minimum problem (in δx and the slack variable u)

$$\begin{aligned} (\delta x, u) = \arg \min_{\delta x, u} & \|F_\nu \delta x - (y_\nu - F_\nu x_M)\|_2^2 \\ & + \lambda_1 \|u - \delta x\|_2^2 + \lambda_2 \|u\|_1 \end{aligned} \quad (7)$$

This equation is iteratively solved for δx (with fixed u) by means of Conjugate Gradient and analytically by soft threshold for u (with fixed δx). At each iteration the data is updated by adding the data residual computed by solving the forward problem.

In both KOMP and the split-Bregman-based approach some regularization parameters must be optimally fixed (the integer number K for KOMP and the regularization parameters λ_1 and λ_2 for ℓ_1 minimization). In the simulated experiments, we applied an optimality criterion, i.e. we minimized the root mean square error between the parameterized reconstructions and the ground truth. In the application against a set of experimental data, we chose for these parameters values of the same order of magnitude as the ones obtained in the simulations and exploited the notable robustness of the reconstruction with respect to variation in this parameters.

IV. NUMERICAL EXAMPLES

We considered two numerical tests for the validation of this sliding window / compressed sensing approach (SWCS from now on) to MRI. The first test aims at determining the amount of spatial resolution that can be recovered thanks to compressed sensing. The second test is to evaluate the overall accuracy of the imaging process in the case of a digital phantom.

A. Test 1: spatial resolution

Our imaging model is made of two identical 2D Gaussian functions with same standard deviation σ , and centered at

$$\mu_y = 0 \quad \mu_x = \pm v \cdot t, \quad (8)$$

where (0,0) is the center of the image. We consider three different velocity values equal to 0.032, 0.064 and 0.128 pixel per frame, with 1000 frames $t \in [-500, 500]$ and five values of $\sigma = 2, 4, 6, 8, 10$. The signal was sampled using radial trajectories separated by the *golden angle* [23]. Each trajectory, corresponding to one time point, sampled 512 k-space points at twice the Nyquist ratio. Images were reconstructed using 305 projections for estimates and 72 projections for residuals.

In the analysis of the reconstructed images we measured (see Figure 1):

- The Full Width at Half Maximum (FWHM) at the first reconstructed frame.
- The frame t_0 at which the grey level at the mid point between the *approaching* two Gaussian functions is equal to half maximum.
- The frame t_1 at which the grey level at the mid point between the two *parting* Gaussian functions is equal to half maximum.
- The last frame $t_2 < 0$ at which the two Gaussian peaks can be distinguished.
- The first frame $t_3 > 0$ at which the two Gaussian peaks can be distinguished again.

The FWHM values for all σ values are in Figure 2; the values of t_0 and t_2 are in Figure 3. As expected, the values of t_1 and t_3 are essentially symmetrical with respect to t_0 and t_2 respectively, and are not shown. The figures are obtained

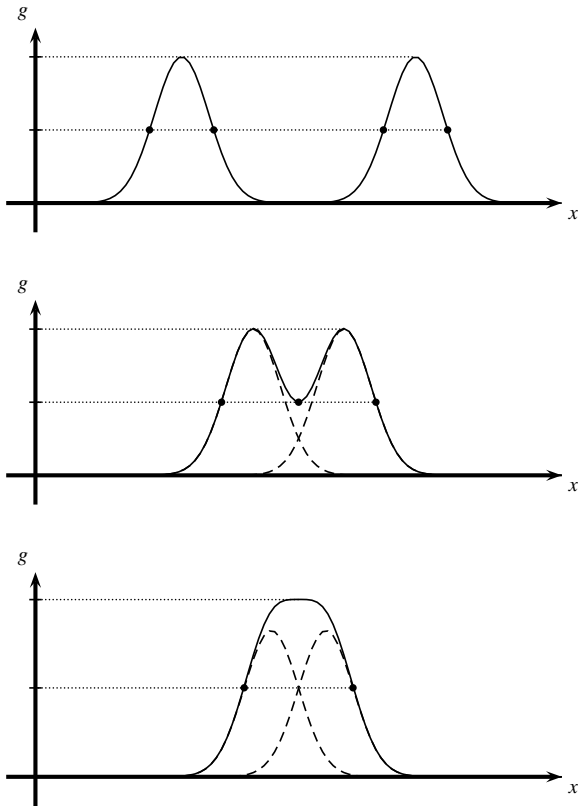


Fig. 1. Gaussians profiles at three key time points: 1a fully separated Gaussians at $t = 0$; 1b unresolved Gaussians at $t = t_0$ and $t = t_1$; 1c Fully superimposed Gaussians at $t = t_2$ and $t = t_3$. In 1b and 1c The dashed line represents the individual Gaussians, the solid line is the sum of the two

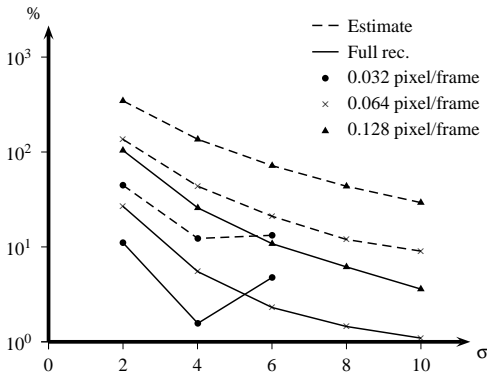


Fig. 2. Measures of FWHM of the Gaussians in estimates and fully reconstructed images. The plot represents relative percentage errors between theoretical values and measures. Data for $\alpha = 0.032$ pixel/frame at $\sigma = 8$ and 10 pixels are not available, since Gaussians are not resolved at any time frame in these experiments.

by using ℓ_1 -optimization but the results provided by KOMP are analogous: in both cases the use of compressed sensing improves the spatial resolution of the reconstruction (and, accordingly, times t_0 and t_2 decrease). As expected, this effect is more significant for higher values of the speed, i.e. when motion blur is more intense.

TABLE I
RMSE FOR TWO SAMPLE FRAMES OF THE SHEPP-LOGAN EXPERIMENT.

152th time frame	p = 0.01	p = 0.02	p = 0.03	p = 0.04
estimate	0.084	0.15	0.22	0.32
KOMP	0.083	0.13	0.16	0.21
Split-Bregman	0.083	0.13	0.16	0.21

600th time frame	p = 0.01	p = 0.02	p = 0.03	p = 0.04
Estimate	0.088	0.16	0.25	0.39
KOMP	0.089	0.14	0.16	0.24
Split-Bregman	0.088	0.14	0.14	0.24

B. Test 2: image quality

For this experiment we considered the Shepp-Logan three-dimensional digital phantom and simulated one-dimensional motion along the direction orthogonal to the image plane. The pixel displacement is

$$d = \Delta x \cdot p, \tag{9}$$

where Δz is the slice thickness and the parameter p mimics the motion velocity. In our applications we assumed $p = 0.01, 0.02, 0.03, 0.04$. To avoid inverse crime, data were generated directly in k-space, using the analytical formula for the Fourier transform of the piecewise function modeling the phantom [24], [25]. We used the same trajectories as in the previous example and time sampling has been chosen in such a way that at $t = 0$ the imaging plane is at the center of the phantom. The measurements in the k-space were affected by Gaussian noise with standard deviation $\sigma = 5 \times 10^{-4}$ times the signal maximum. The results of this experiment are in Table I, containing the root mean square error (RMSE) for the blurred estimate and for SWCS with KOMP and the split-Bregman algorithm, corresponding to two specific time points. Further, Figure 4 visually illustrates the reconstructions for just two values of p , namely $p = 0.01, 0.04$. Both the table and the figure show that the SWCS improves the quality of the reconstruction, particularly for high values of p while the improvement is negligible at low speed, when the correction demand is low. We point out that in both the images in the figure and the computation of the reconstruction errors we applied a binary mask that excludes the background.

V. APPLICATION TO ORTHOPEDIC IMAGING

We scanned a human subject using a 0.5 T MRI system with an open U-shaped magnet (Mr Open, Paramed Medical System, Genova, Italy). We performed cervical spine imaging using a two-channel dedicated coil according to the following parameters: TE/TR 7.3/20 ms; FA 30°; sagittal plane; FOV 300 mm; 512 samples; sampling bandwidth ± 50 kHz; slice thickness 6 mm; 1000 time frames. With these parameters we achieved a time sampling of 50 frames per second. The subject was instructed to flex and extend his neck during the acquisition at 3 cycles per minute. Figure 5 presents the estimate provided by conjugate gradient when applied against the whole data set (corresponding to 305 trajectories), the residual restored by compressed sensing when using just 72 trajectories (this is the implementation based on ℓ_1 optimization) and the

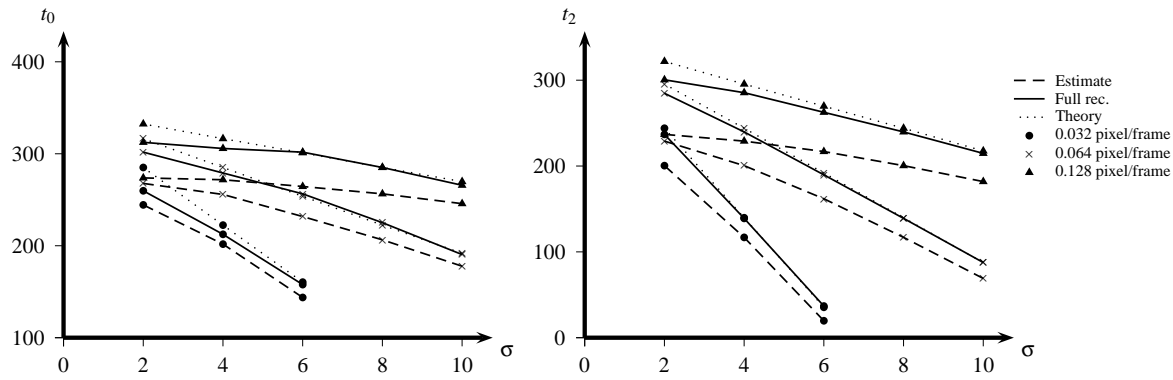


Fig. 3. Measures of t_0 (left) and t_2 (right) for estimates and full reconstructions, in comparison with theoretical values. Data for $v = 0.032$ pixel/frame at $\sigma = 8$ and 10 pixels are not available, since Gaussians are fully superimposed at any time frame in these experiments.

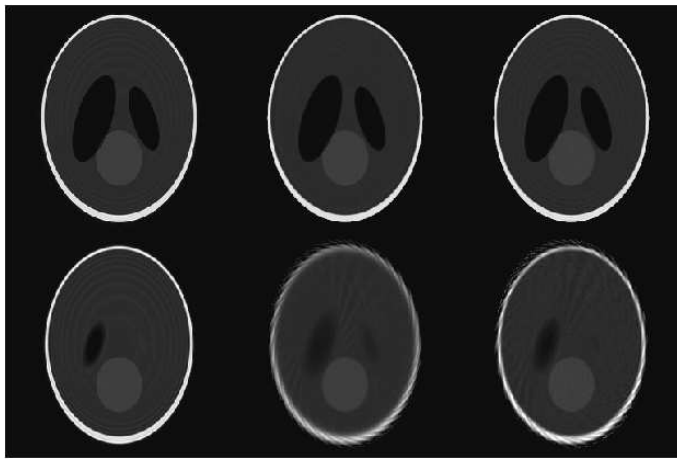


Fig. 4. Shepp-Logan images for time frame number 300 for two different speeds. Top row is speed $p = 0.01$; bottom row is speed $p = 0.02$. Left column is ground truth images; central column is estimate images; and Right column is the final reconstruction, sum of estimates and CS residuals. While on lower speed the contribution of CS is minimal, due to low blurring levels, resolution improvements are evident at higher speed. Moreover at higher speed the left ventricle is slightly visible on estimates, but is clearly an artifact; on the final images this artifact disappears.

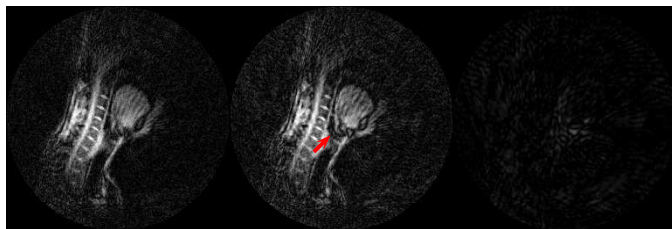


Fig. 5. Sample frame of the volunteer scan. The image on the left is the estimate; the central image is the full reconstruction; the image on the right is the residual. The most significant improvement can be seen in the region below the tongue, marked with the arrow.

sum of the two. This figure shows that, particularly in the region below the tongue, SWCS is able to recover some high resolution details hidden in the reconstruction provided by the conjugate gradient estimate.

VI. CONCLUSIONS

The present paper describes a novel strategy for acquisition and reconstruction of images from dynamic MRI data. The approach exploits a sliding window paradigm for the recording of trajectories in k-space, a standard regularization method for the reconstruction of an initial estimate corresponding to a complete data set and compressed sensing techniques for the reconstruction of the residual images in correspondence of narrow time intervals. We showed that this strategy is reliable for improving both the achievable spatial resolution and the overall reconstruction quality, even in the case of data acquired with low-field systems. The strategy does not significantly depend on the kind of sparsity enhancing technique applied during the compressed sensing step. From a computational viewpoint, we realized that, in the numerical tests performed, the optimal values for K in KOMP is rather high. Accordingly, the optimal value of the regularization parameter controlling the ℓ_1 penalty term in split-Bregman is rather small. This suggests the need of a more systematic investigation of the interplay between the roles of sparsity and sliding window acquisition in the image reconstruction process. Finally, in order to systematically study the applicability power of this approach it is now necessary to validate its performances against experimental data acquired in clinical contexts.

ACKNOWLEDGMENT

Cristian Toraci is supported by a PO CRO FSE 2007/13 Asse IV grant from Regione Liguria, Italy. The experimental part described in the paper has been performed in Vancouver, at the Center for Hip Health and Mobility and was supported by an operating grant from the Canadian Institutes of Health Research.

REFERENCES

- [1] P. Mansfield, "Multi-planar image formation using NMR spin echoes," *J. Phys. C Solid State*, vol. 10, no. 3, pp. L55–L58, Feb. 1977. [Online]. Available: <http://dx.doi.org/10.1088/0022-3719/10/3/004>
- [2] I. L. Pykett Richard and R. Rzedzian, "Instant images of the body by magnetic resonance," *Magn. Reson. Med.*, vol. 5, no. 6, pp. 563–571, 1987. [Online]. Available: <http://dx.doi.org/10.1002/mrm.1910050607>

- [3] G. C. McKinnon, "Ultrafast interleaved gradient-echo-planar imaging on a standard scanner," *Magn. Reson. Med.*, vol. 30, no. 5, pp. 609–616, 1993. [Online]. Available: <http://dx.doi.org/10.1002/mrm.1910300512>
- [4] M. Blaimer, F. Breuer, M. Mueller, R. M. Heidemann, M. A. Griswold, and P. M. Jakob, "SMASH, SENSE, PILS, GRAPPA: how to choose the optimal method," *TMRI*, vol. 15, no. 4, pp. 223–236, Aug. 2004. [Online]. Available: <http://view.ncbi.nlm.nih.gov/pubmed/15548953>
- [5] K. P. Pruessmann, "Encoding and reconstruction in parallel MRI," *NMR Biomed.*, vol. 19, no. 3, pp. 288–299, 2006. [Online]. Available: <http://dx.doi.org/10.1002/nbm.1042>
- [6] J. Tsao, B. Behnia, and A. G. Webb, "Unifying linear prior-information-driven methods for accelerated image acquisition," *Magn. Reson. Med.*, vol. 46, no. 4, pp. 652–660, 2001. [Online]. Available: <http://dx.doi.org/10.1002/mrm.1242>
- [7] D. L. Donoho, "Compressed sensing," *IEEE T. Inform. Theory*, vol. 52, no. 4, pp. 1289–1306, Apr. 2006. [Online]. Available: <http://dx.doi.org/10.1109/tit.2006.871582>
- [8] E. J. Candes, J. Romberg, and T. Tao, "Robust uncertainty principles: exact signal reconstruction from highly incomplete frequency information," *IEEE T. Inform. Theory*, vol. 52, no. 2, pp. 489–509, 2006.
- [9] M. Lustig, D. Donoho, and J. M. Pauly, "Sparse MRI: The application of compressed sensing for rapid MR imaging," *Magn. Reson. Med.*, vol. 58, no. 6, pp. 1182–1195, Dec. 2007. [Online]. Available: <http://dx.doi.org/10.1002/mrm.21391>
- [10] U. Gampfer, P. Boesiger, and S. Kozerke, "Compressed sensing in dynamic MRI," *Magn. Reson. Med.*, vol. 59, no. 2, pp. 365–373, 2008. [Online]. Available: <http://dx.doi.org/10.1002/mrm.21477>
- [11] H. Jung, K. Sung, K. S. Nayak, E. Y. Kim, and J. C. Ye, "k-t FOCUSS: A general compressed sensing framework for high resolution dynamic MRI," *Magn. Reson. Med.*, vol. 61, no. 1, pp. 103–116, 2009. [Online]. Available: <http://dx.doi.org/10.1002/mrm.21757>
- [12] Z.-P. Liang and P. C. Lauterbur, "An efficient method for dynamic magnetic resonance imaging," *IEEE T. Med. Imaging*, vol. 13, no. 4, pp. 677–686, Dec. 1994. [Online]. Available: <http://dx.doi.org/10.1109/42.363100>
- [13] D. Le Gall, "MPEG: a video compression standard for multimedia applications," *Commun. ACM*, vol. 34, no. 4, pp. 46–58, Apr. 1991. [Online]. Available: <http://dx.doi.org/10.1145/103085.103090>
- [14] L. Feng, R. Grimm, K. T. Block, H. Chandarana, S. Kim, J. Xu, L. Axel, D. K. Sodickson, and R. Otazo, "Golden-angle radial sparse parallel MRI: Combination of compressed sensing, parallel imaging, and golden-angle radial sampling for fast and flexible dynamic volumetric MRI," *Magn. Reson. Med.*, p. n/a, Oct. In press. [Online]. Available: <http://dx.doi.org/10.1002/mrm.24980>
- [15] M. A. Bernstein, K. F. King, and X. J. Zhou, *Handbook of MRI Pulse Sequences*, 1st ed. Academic Press, Sep. 2004. [Online]. Available: <http://www.worldcat.org/isbn/0120928612>
- [16] M. Usman, D. Atkinson, F. Odille, C. Kolbitsch, G. Vaillant, T. Schaeffter, P. G. Batchelor, and C. Prieto, "Motion corrected compressed sensing for free-breathing dynamic cardiac MRI," *Magn. Reson. Med.*, vol. 70, no. 2, pp. 504–516, Aug. 2013. [Online]. Available: <http://dx.doi.org/10.1002/mrm.24463>
- [17] J. A. Tropp, "Greed is good: algorithmic results for sparse approximation," *IEEE T. Inform. Theory*, vol. 50, no. 10, pp. 2231–2242, Oct. 2004. [Online]. Available: <http://dx.doi.org/10.1109/tit.2004.834793>
- [18] S. J. Riederer, T. Tasciyan, F. Farzaneh, J. N. Lee, R. C. Wright, and R. J. Herfkens, "MR fluoroscopy: Technical feasibility," *Magn. Reson. Med.*, vol. 8, no. 1, pp. 1–15, 1988. [Online]. Available: <http://dx.doi.org/10.1002/mrm.1910080102>
- [19] A. C. Gilbert, S. Muthukrishnan, and M. J. Strauss, "Approximations of functions over redundant dictionaries using coherence," in *SODA '03 Proceedings of the fourteenth annual ACM-SIAM symposium on Discrete algorithms*. Society for Industrial and Applied Mathematics, 2003, pp. 243–252.
- [20] D. Needell and R. Vershynin, "Signal Recovery From Incomplete and Inaccurate Measurements Via Regularized Orthogonal Matching Pursuit," *IEEE J. Sel. Top. Sig. Proc.*, vol. 4, no. 2, pp. 310–316, Apr. 2010. [Online]. Available: <http://dx.doi.org/10.1109/jstsp.2010.2042412>
- [21] D. Needell and J. A. Tropp, "CoSaMP: Iterative signal recovery from incomplete and inaccurate samples," *Appl. Comput. Harmon. A.*, vol. 26, no. 3, pp. 301–321, May 2009. [Online]. Available: <http://dx.doi.org/10.1016/j.acha.2008.07.002>
- [22] T. Goldstein and S. Osher, "The Split Bregman Method for L1-Regularized Problems," *SIAM J. Imaging Sci.*, vol. 2, no. 2, pp. 323–343, Apr. 2009. [Online]. Available: <http://dx.doi.org/10.1137/080725891>
- [23] S. Winkelmann, T. Schaeffter, T. Koehler, H. Eggers, and O. Doessel, "An Optimal Radial Profile Order Based on the Golden Ratio for Time-Resolved MRI," *IEEE T. Med. Imaging*, vol. 26, no. 1, pp. 68–76, Jan. 2007. [Online]. Available: <http://dx.doi.org/10.1109/tmi.2006.885337>
- [24] M. Guerquin-Kern, L. Lejeune, K. P. Pruessmann, and M. Unser, "Realistic Analytical Phantoms for Parallel Magnetic Resonance Imaging," *IEEE T. Med. Imaging*, vol. 31, no. 3, pp. 626–636, Mar. 2012. [Online]. Available: <http://dx.doi.org/10.1109/tmi.2011.2174158>
- [25] C. G. Koay, J. E. Sarlls, and E. Özarslan, "Three-dimensional analytical magnetic resonance imaging phantom in the Fourier domain," *Magn. Reson. Med.*, vol. 58, no. 2, pp. 430–436, Aug. 2007. [Online]. Available: <http://dx.doi.org/10.1002/mrm.21292>